

# MULTIDISCIPLINARY OPTIMIZATION OF TRUSS-BRACED WING LAYOUT

Ke-Shi ZHANG \*, Abu BAKAR\*, Peng-Bo JI\*, Zhong-Hua Han\*, Xiao-Peng Li\*  
\* School of Aeronautics, Northwestern Polytechnical University, Xi'an, 710072, P.R. China  
zhangkeshi@nwpu.edu.cn

**Keywords:** multidisciplinary design optimization, strut-braced wing, truss-braced wing, wing/strut/jury interference drag

## Abstract

*Innovative configurations such as truss-braced wing (TBW) offer the potential of greatly reducing the fuel consumption of future greener transport aircraft. Previous study suggests that the benefit of a TBW configuration needs to be fully exploited by multidisciplinary design optimization (MDO). This paper conducted a MDO study of the TBW configurations by integrating the aerodynamic and structure disciplines. For aerodynamic discipline, the induced drag, wave drag, friction drag as well as interference drag due to wing, strut and jury is investigated; for structural discipline, the box-beam model is used and full-stress optimization is utilized for sizing. The aerodynamic/structural analysis is integrated within an efficient surrogate-based optimization framework and the multi-objective optimization of the wing, strut and jury is performed. The Pareto front results show that TBW with 2 juries is the most effective configuration with respect to the aerodynamic lift-to-drag ratio and structural weight.*

## 1 Introduction

As the conventional transport aircraft configuration characterized by cantilevered wings has already reached to a maturity level, it is for the designers to make a significant improvement, to meet the demand of new generation transport design. Innovative airframe designs have to be explored to achieve a substantial increase in lift-to-drag ratio for a given vehicle weight.

The truss-braced (or strut-braced) wing configuration is a promising innovative design that was proposed by NASA as one of the N+3

(2030-2035) generation aircraft concepts [1]. Truss-braced wing (TBW) configuration has received increasing attention due to its great potential to reduce the fuel consumption of aircraft. The benefits of TBW configuration can be explained by the following aspects: First, the truss provides bending load alleviation to the wing, allowing for a decreased thickness to chord ratio, an increased span and usually a reduction of wing weight; second, the thinner wing leads to lower transonic wave drag, and the larger wing span results in reduction of the induced drag. In addition, these favorable features allow for smaller wing sweep, which may unlock the limit of attaining natural laminar flow over traditional transonic wing; third, the engine size can be reduced due to the decreased weight and increased aerodynamic efficiency; last, the drag reduction means fewer fuel consumption. Thus the TBW configuration is regarded as one of the promising configurations of future green aircraft.

The idea of TBW configuration was proposed by Pfenninger in the early 1950s [2]. However, the early work focused on structure or aerodynamics discipline separately. As tight coupling exists between structure and aerodynamics, the full potential of TBW configuration needs to be reinvestigated in a multidisciplinary way. Mason et al. have conducted series of work on TBW configuration since 1997 [3], which suggest that multidisciplinary analysis and optimization of TBW configuration has potential of fully exploiting its benefit [4][5].

For design of a TBW wing, multidisciplinary design optimization (MDO) plays a critical role in fully exploiting its benefit

[5][6], due to the fact that the tight couplings exist among different disciplines, such aerodynamics, structure, weight, propulsion, etc.

This paper aims to perform an aerodynamic/structural integrated optimization of a TBW configuration layout. The wing/strut/jury thickness and intersection locations, wing span and sweep angles of wing/strut is optimized, to achieve an optimal performance, while considering both aerodynamic and structural effect. By comparison of the optimal concepts of TBW configurations with the traditional cantilever wing, the benefit of TBW is evaluated.

## 2 Modeling and Analysis

### 2.1 General Statement of Design Problem

The TBW aircraft is designed similar to A320-200 which flies a range of 5700km at M0.78 with 150 passengers. The wing is of span 34.1m and aspect ratio 9 that is a typical value for the civil airliners.

In a strut-braced wing (SBW) design, a strut is installed between the wing and fuselage. This strut can support high aspect ratio wing without any weight penalty. There are certain benefits associated with high aspect ratio wing. To further increase these benefits, a jury can be used between the wing and the strut. The number to juries may be 1 or more. These modified SBW designs are called truss-braced wing, TBW-n (n is the number of juries). SBW, TBW-1 and TBW-2 are shown in Figure 1.

Three most critical load cases, 1g cruise, 2.5g climb, -1g maneuver, are considered in the design. Apart from the aerodynamic loads, engine weight and fuel loading is also considered.

In the following text it should be noted that, the wing weight for a cantilever wing means the bending material weight, and the wing weight for a TBW means the bending weight plus the truss-members weight.

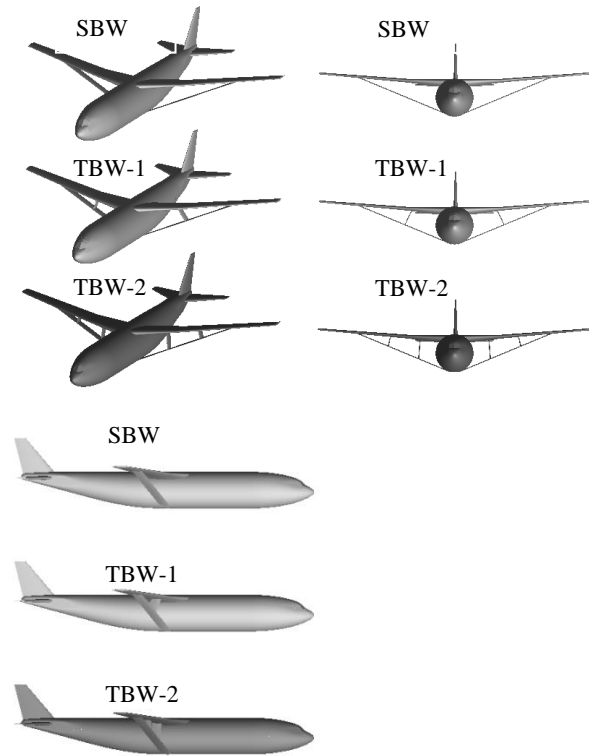


Figure 1 SBW, TBW-1 and TBW-2 designs [6]

### 2.2 Structural Modeling and Analysis

The structure is idealized as a box-beam model (Figure 2). This model is made up of web and upper and lower skin panels for carrying bending and torsion moments. The wing structure is simplified as a box-beam with ten variable cross-sections.



Figure 2 Box-beam model for wing section

The beam with variable cross sections is shown in

Figure 3. ANSYS is applied in the FEM analysis. Full-stress optimization is programmed for wing box sizing. Assuming same thickness for front and rear spar web, and for upper and lower skin, the sizing variables of full-stress optimization are listed in

Table 1.

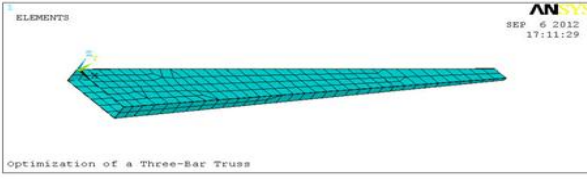


Figure 3 Box beam model for wing

Table 1 Variables for full stress optimization

Variables	number
Skin thickness variables of wing box ( $t_s$ )	1 - 10
Web thickness variables of wing box ( $t_w$ )	11 - 20
Cross sectional area of strut or truss members	1 for each strut or jury

### 2.3 Aerodynamic Modeling and Analysis

A transonic vortex lattice method is used to predict the induced drag and span-wise load distribution. The friction/form drag is calculated based on the wetted area and using the prediction of skin friction models as well as form-factor estimation. The wave drag is modeled by Korn Equation.

#### 2.3.1 Induced drag

In the current study, Multiple Lifting Line code [7] is used to predict the induced drag. Firstly LAMDES [8] is used to calculate the twist distribution for minimum induced drag. Then the twist distribution is input into Multiple Lifting Line code for induced drag prediction. Multiple Lifting Line code also has the capability to analyze the control surfaces like ailerons and flaps. Hence it can be later applied in more detailed analysis. LAMDES is also for calculation of the sectional load distribution, which will be applied on the wing for weight calculation of the bending material.

The twist distribution for reference wing at mach 0.78 and lift coefficient 0.67 is presented in Figure 4. The wing is washed-out to decrease the loads on the tip. It will help producing elliptical loading and reduce the chance of stall at wing tip. A small peak near the wing kink is because of sudden change in chord along the span. The twist increases a little to compensate for the loss of lift. Similar results are also obtained in [9].

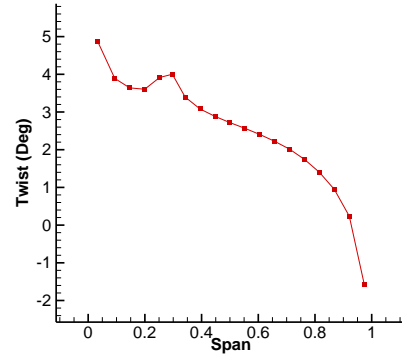


Figure 4 Twist distribution by LAMDES [8]

#### 2.3.2 Wave drag

Wave drag is modeled using Korn equation extended to sweep wings. The equation is presented below.

$$M_{dd} = \frac{\kappa_A}{\cos \Lambda} - \frac{t/c}{\cos \Lambda} - \frac{C_L}{10 \cos \Lambda} \quad (1)$$

$$M_{crit} = M_{dd} - \left( \frac{0.1}{80} \right)^3 \quad (2)$$

Where  $M_{dd}$  is the drag divergence mach number,  $t/c$  is the thickness to chord ratio,  $C_L$  is the sectional lift coefficient and  $\kappa_A$  is airfoil technology factor or Korn factor.  $M_{crit}$  (critical mach number) from Eq.(2) can be then used to calculate the wave drag coefficient from the following relation [10]

$$C_{D_{wave}} = 20(M - M_{crit})^4 \frac{S_{strip}}{S_{ref}} \quad (3)$$

#### 2.3.3 Skin friction drag

For current study friction/form drag is based on flat plate skin friction coefficients. The following relationship is used to calculate the friction/form drag coefficient.

$$C_{D,F} = C_F FF \frac{S_{wet}}{S_{ref}} \quad (4)$$

Where  $C_F$  is a flat-plate skin-friction coefficient,  $FF$  is the form factor of the component, and  $S_{wet}$  and  $S_{ref}$  are the wetted and reference areas, respectively.

Code written by W. H. Mason [11] is used for friction/form drag prediction. To estimate the transition Reynolds number on the wing, Technology Factor definition used in [12] is used. Technology factor of 0 represents the conventional airfoils, whereas technology factor of 1 represents natural laminar flow airfoils.

The above codes are validated with DLR F4 wing configuration. DLR F4 is a standard wing body configuration. The experimental data is available for wide range of Reynolds number and lift coefficient. Here experimental data for Reynolds number  $3 \times 10^6$  and lift coefficient 0.5 is used for validation. Two cases are considered i.e. mach 0.6 and mach 0.75. For mach 0.6 only induced drag and skin friction models are used. Wave drag model is added for mach 0.75. Drag polars for both mach numbers are presented in Figure 5. For DLR F4 validation transition location is fixed at 25% of the chord and Korn factor is 0.91.

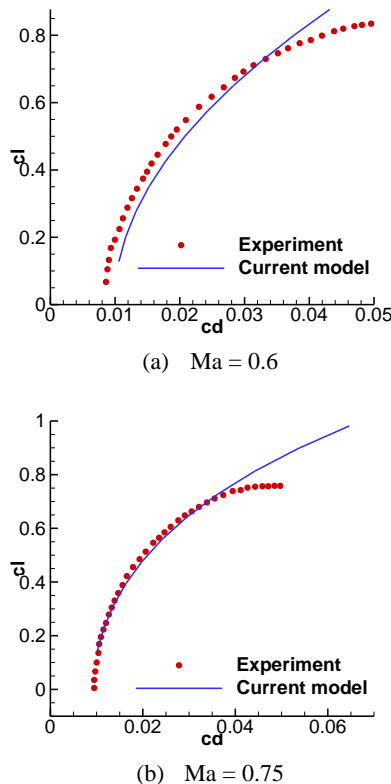


Figure 5 Comparison of predicted drag polar for DLR F4 wing-body configuration at Reynolds number of 3 Million, and lift coefficient of 0.5: (a) mach 0.6, (b) mach 0.75

### 2.3.4 Interference drag

For predicting the interference drag caused by different intersections, i.e., wing-strut, strut-strut and strut-fuselage intersections, ICEM software is used to generate structured mesh and Fluent software is used to simulate the inviscid transonic flow around the intersection configurations mentioned above.

#### Strut/wing interference drag

Study of strut-wing interference drag is based on DLR-F4 wing body configuration, for mach 0.78 according to the cruise Mach number of A320-200 aircraft. After some simulation, it was concluded that at alpha  $-1.5$ , lift coefficient of 0.5 is achieved. Next a strut is attached to wing. The airfoil of the strut is NACA 64A-010 symmetric airfoil with a thickness to chord ratio of 10. Initially the strut is parallel to the longitudinal axis of aircraft, i.e. the strut will also face  $-1.5$  deg alpha. Hence the strut will experience negative loads. Grid on symmetry plane, wing and strut is shown in Figure 6.

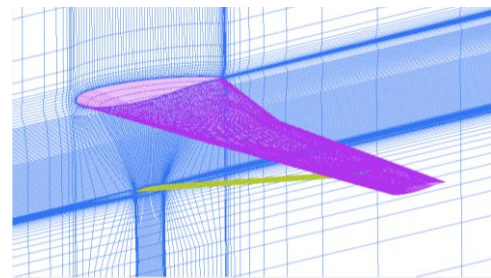


Figure 6 Symmetry plane, wing and strut grid for inviscid computation of wing/strut interference drag

The strut airfoil is a symmetric airfoil but foot print (intersection of strut with wing) of strut on lower surface of the wing is highly cambered. The footprint of wing-strut intersection is display in Figure 7.

Now the flow velocity is expected to increase near the wing-strut intersection. Firstly it is because the air is forced through a narrow channel between the upper surface of strut and lower surface of wing. Therefore the velocity increases. Secondly the footprint of the strut-wing intersection is highly cambered. The local mach number near intersection will exceed 1. Hence at the intersection there will be a strong shock wave.

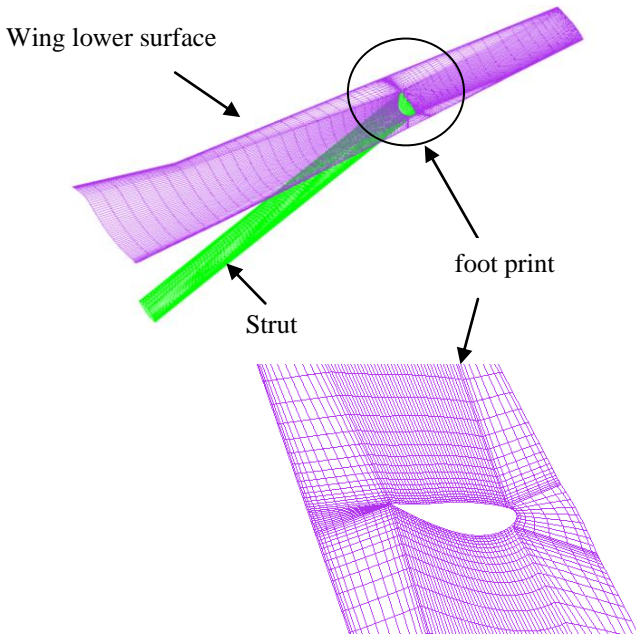


Figure 7 Footprint of wing-strut intersection

Arc-shaped strut-wing intersection can help to decrease the interference drag. An arc-shaped intersection provides larger area for the air to flow through. Also arc-shaped strut can also help to avoid buckling of strut under negative wing loads. Arc-shaped strut study is also performed for DLR F4 wing with three different arc radiuses, 10 mm, 20 mm and 30 mm. Front view of wing with straight and arc-shaped struts is shown in Figure 8. All the struts are also rotated by an angle of 1.5 degrees for maximum lift recovery.

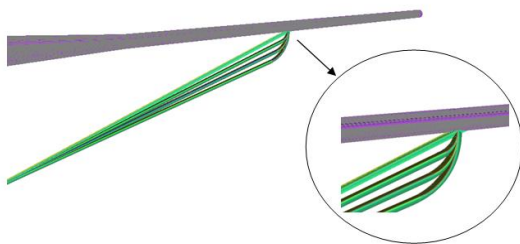


Figure 8 Wing with straight and arc-shaped struts

Lift and drag coefficients for straight and arc-shaped strut are listed in Table 2. Zero-deg strut decreases the lift coefficient. Rotating the strut recovers most of the lift but increases the interference drag. Larger radius with 1.5 deg strut shows minimum interference drag penalty.

Table 2 Lift and drag coefficient comparison for straight and arc-shaped strut

Configuration	$C_L$	$C_D$	$\Delta C_D$
Wing alone	0.501	0.0148	-----
Wing with strut (0 deg)	0.4561	0.0167	0.0019
Wing with Strut (1.5 deg)	0.4817	0.0189	0.0041
Wing with Strut R1 (1.5 deg)	0.4879	0.0186	0.0038
Wing with Strut R2 (1.5 deg)	0.4883	0.0182	0.0034
Wing with Strut R3 (1.5 deg)	0.4888	0.0176	0.0028

### Strut/fuselage interference drag

For strut-fuselage interference drag prediction, un-swept strut between two parallel side walls is considered (Figure 9). Two airfoils are considered for this analysis, NACA 64A-006 and NACA 64A-010. The distance between the two walls is set to five times the chord of strut airfoil. Here only inviscid effect is considered and the interference due to viscous effect will be considered in the future study.

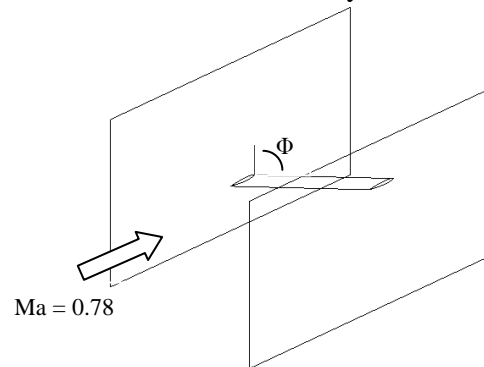


Figure 9 Strut arrangement between two side walls

As strut is placed between two side walls, twice the interference drag is calculated as the difference between the strut with and without the effect of wall. Analysis is carried out for three intersection angles,  $\Phi=90, 60$  and  $30$  degrees. The drag coefficient is non-dimensionalized by reference area of  $A_{320}$ .

The variation of interference drag coefficient with strut-fuselage intersection angle is presented in Figure 10. The interference drag for NACA 64A-006 is almost same for intersection angle  $90$  and  $45$  degrees. It is

because there is no shock wave on the strut. For thicker strut airfoil, NACA 64A-010, the drag increases rapidly with increase in intersection angle.

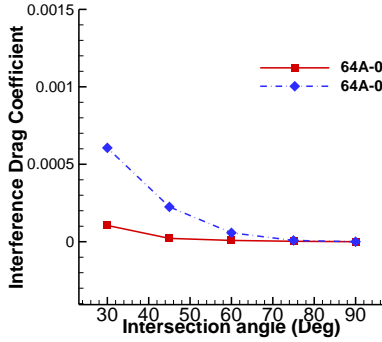


Figure 10 Interference drag increase with intersection angle

### Strut/strut interference drag

The procedure to estimate interference drag for strut-strut intersection is explained here. Firstly inviscid analysis is carried out for 2D airfoil. The drag of the airfoil is named as “drag-2D”. Next strut-strut intersection arrangement is enclosed in the computational domain as shown in Figure 11. The shaded sides are treated as inviscid walls and pressure far field boundary conditions are applied to the blank sides. The flow field extends to 5 times the chord upstream, downstream, above and below the strut-strut intersection. Inviscid drag of this arrangement is named as “drag-3D”. Now the 2D-drag is multiplied by total length of the strut to get “equivalent drag-3D”. Equivalent drag-3D is subtracted from drag-3D to get interference drag. Similar methodology was also adopted in [13].

Similar to strut-wall study, the strut airfoils considered are NACA 64A-006 and NACA 64A-010. Intersection angle is varied from 50 to 90 deg.

Interference drag coefficient increase with intersection angle of the strut is also presented in Figure 12 below. The drag coefficient is non-dimensionalized by reference area of A320. Even for intersection angle 90, NACA 64A-010 strut has much higher drag coefficient than 64A-006 strut. It is because thicker strut also produces shock wave even for 90 deg intersection angle.

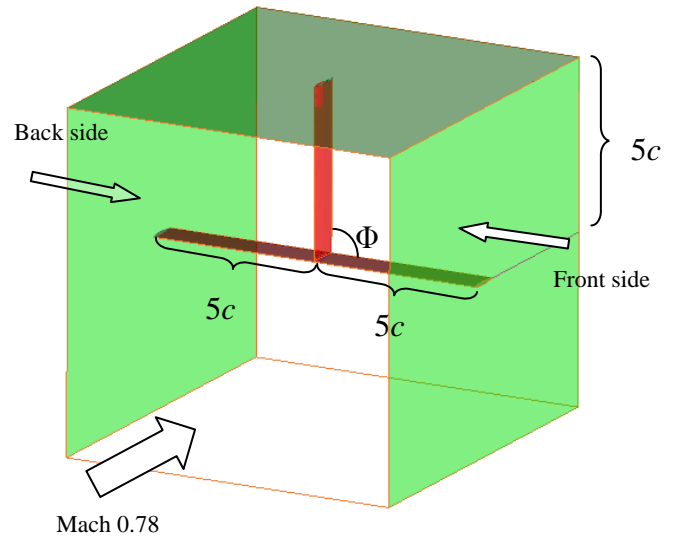


Figure 11 Strut/strut arrangement in computational domain

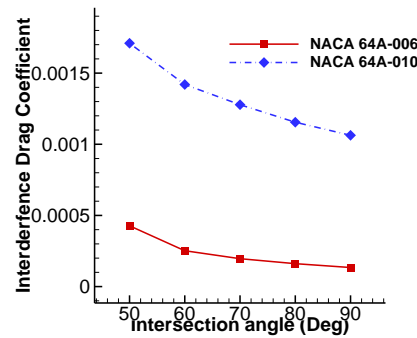


Figure 12 Interference drag coefficient with intersection angle

### Fairing factors

Interference drag models discussed above show that wing-strut intersection is major contributor to the interference drag. The interference drag of strut/fuselage and strut/strut intersection is relatively small as compared to wing-strut interference drag.

Wing-strut interference drag can be reduced by using a fairing at the intersection. As SBW and TBW are N+3 generation designs, aggressive fairing factor should be used. According to literature, fairing can reduce interference drag by 98%. Hence aggressive fairing factor is 0.02. Similarly conservative and conventional fairing factors are 0.1 and 0.2 respectively [14].

**2.4 Optimization Modeling and Optimization Method**

For optimization of cantilever, SBW, TBW-1 and TBW-2 configurations, the objectives of the optimization are to maximize lift-to-drag ratio and minimize the weight of wing, cruising at 0.78 mach at altitude of 12,000 m. Mathematical model of wing optimization is defined below.

$$\begin{aligned}
 & \text{Max } L/D \\
 & \text{min } W_{\text{wing}} \\
 & \text{s.t. } C_L \geq 0.67 \\
 & \quad S_{\text{Ref}} = 122.4
 \end{aligned} \tag{4}$$

During optimization area of wing is kept constant. Hence for wing with higher span than A320, the chords will be reduced. Four design variables are used to define the aerodynamic configuration of the wing, as listed in Table 3.

**Table 3 Design variables for configuration optimization**

Design Variables	Unit	Lower bound	Upper bound
Span	Meter	17.5	23
t/c at root	-	0.06	0.14
t/c at tip	-	0.06	0.14
Sweep	Deg	20	35

For structure discipline alone, full-stress optimization is performed to optimize thickness of skin and of front spar web at ten span stations.

An efficient surrogate-based global optimization tool, SurroOpt [15][16], is employed. Initial samples points are selected by Latin hypercube sampling (LHS) method. The object function and state functions at these points are evaluated by aforementioned aerodynamic and structure analysis method. An initial kriging model (s) [17] is built and a multi-objective Genetic algorithm called NSGA-II [18] is employed to perform the sub optimization to guess the Pareto front. Aerodynamic analysis and structure sizing are carried out at these guess points to obtained new sample points. The kriging model (s) is repetitively updated until the whole optimization process convergent to the real Pareto front solution.

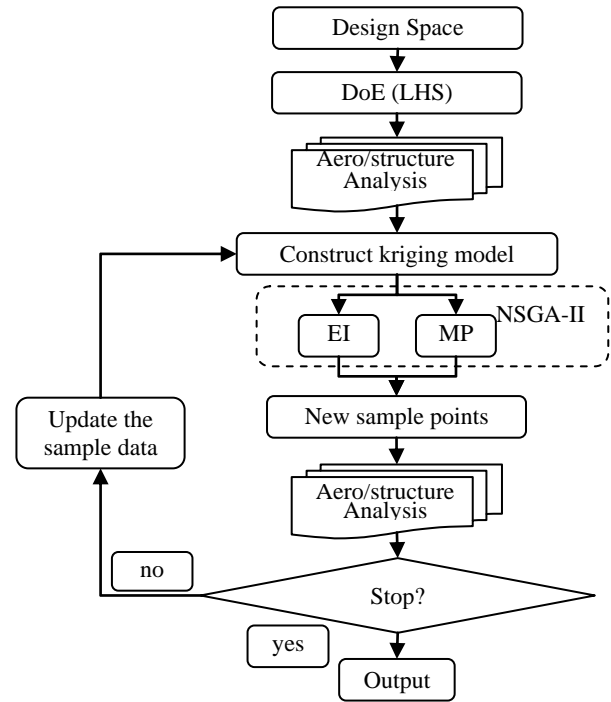


**Figure 13 Flow chart of the surrogate –based optimization**

**3 Results and Discussion**

**3.1 Pareto front and optimum configuration**

For all design configurations, Korn factor is 0.91. Technology factor is 1.0 and maximum chord-wise laminar flow is limited to 70% of the local chord. Aggressive fairing factor of 0.02 is used for wing-strut, strut-fuselage and strut-strut intersections. Pareto fronts of cantilever, SBW, TBW-1 and TBW-2 are presented in Figure 14. It can be concluded that, adding a strut provides weight saving and increases *L/D*. Consider the optimum cantilever design corresponding to *L/D* 29 and weight 2620 Kg. For same *L/D*, the weight of strut braced wing is 2190 Kg. The weight saving offered by SBW is 16%. Similarly for TBW-1 and TBW-2 weight saving is 38% and 45%. At lower *L/D*, it seems that TBW-2 design offers no advantage over TBW-1. At higher *L/D*, TBW-2 design shows considerable weight saving. It is because higher *L/D* corresponds to higher span and strut/jury is more effective at higher span.

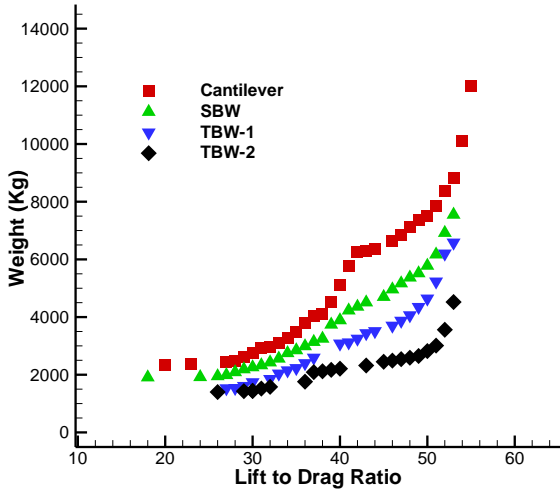
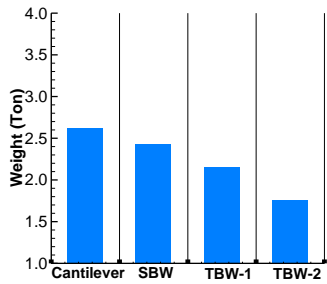
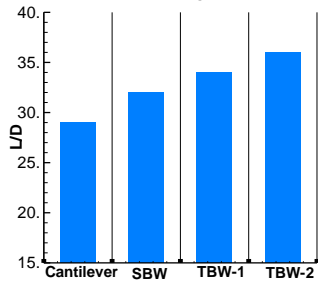


Figure 14 Pareto points of different wing configurations

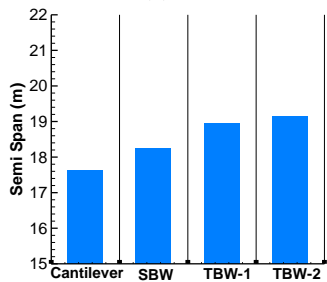
Still taking the optimum cantilever design corresponding to  $L/D$  29 and weight 2620 kg as the baseline, some parameters of the corresponding SBW and TBW designs are compared in Figure 15. Wing weight, aspect ratio, lift to drag ratio, semi span, average thickness and sweep of optimized configurations are presented.



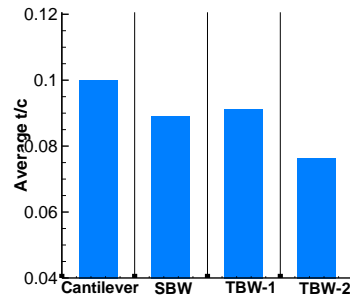
(a) weight



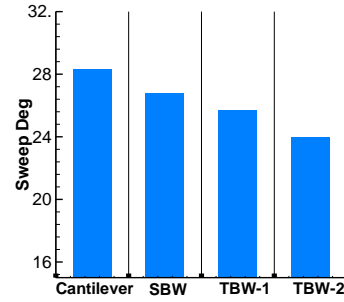
(b) L/D



(c) Span



(d) Average t/c



(e) Leading-edge swept angle

Figure 15 Comparison of baseline and optimized TBW

### 3.2 Aerodynamic trend study of TBW-2 configuration

In the following part, taking the optimal TBW-2 configuration as a reference, a sensitivity study is performed for the various aerodynamic parameters to explore how the aerodynamic considerations affect the optimal design. For each study, one parameter is altered while the others are kept the same as in the baseline design. The parameters including fairing factor, Korn factor, technology factor and chord-wise laminar flow percentage are explored in the following trend study (see Table 4 and Figure 16).

Table 4 Parametric study of TBW-2 wing, baseline, lower and upper values

Parameter	Baseline value	Lower limit	Upper limit
Sweep back angle	24	20	28
Korn factor	0.91	0.87	0.95
Fairing factor	0.02	0.02	0.2
Technology factor	1	0	1
Maximum chord-wise laminar flow	70%	40%	100%

The results of this parameterization can be concluded as following:

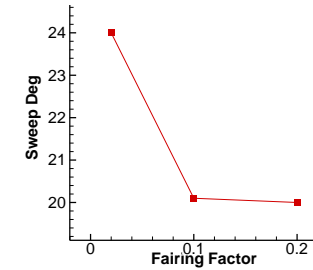
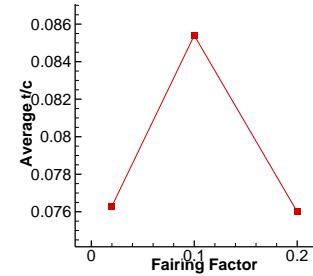
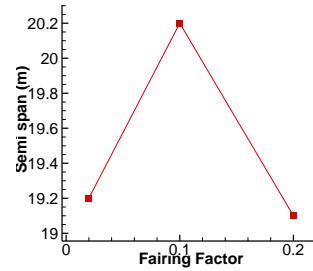
1) As the sweep angle is decreased, the lift to drag ratio also decreases. It is because wave drag increases sharply and skin friction drag remains the same. The laminar flow is only limited to 70% of the chord over the wing. Hence the benefit of laminar flow at lower sweep angle is not fully exploited.

2) As the fairing factor is increased (less effective fairing), the interference drag increases and lift to drag ratio decreases.

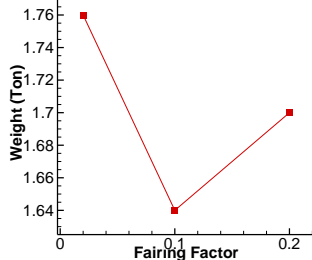
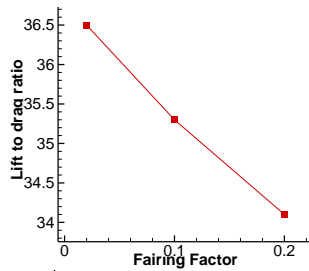
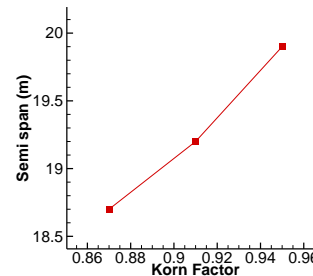
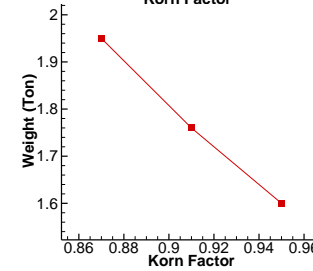
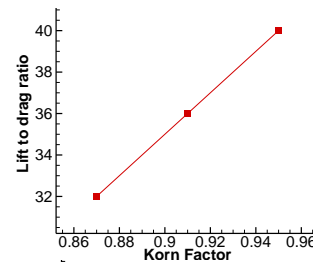
3) Increasing Korn factor (high performance airfoil) decreases the wave drag. The sweep angle is decreased without wave drag penalty. Increase in span also decreases induced drag. Lower sweep and increased span will also allow more laminar flow over the wing.

4) Increasing the technology factor will increase the sweep back angle without skin friction drag penalty and decreases wave drag. Lift to drag ratio increases at the cost of weight.

5) Next generation aircraft will have aggressive laminar flow. Increasing the laminar flow over wing will decrease the sweep angle. Wave drag penalty is compensated by reduction in induced drag because of higher wing span. Considerable increase in lift to drag ratio can be achieved with aggressive laminar flow technology.



(a) Fairing factor trend



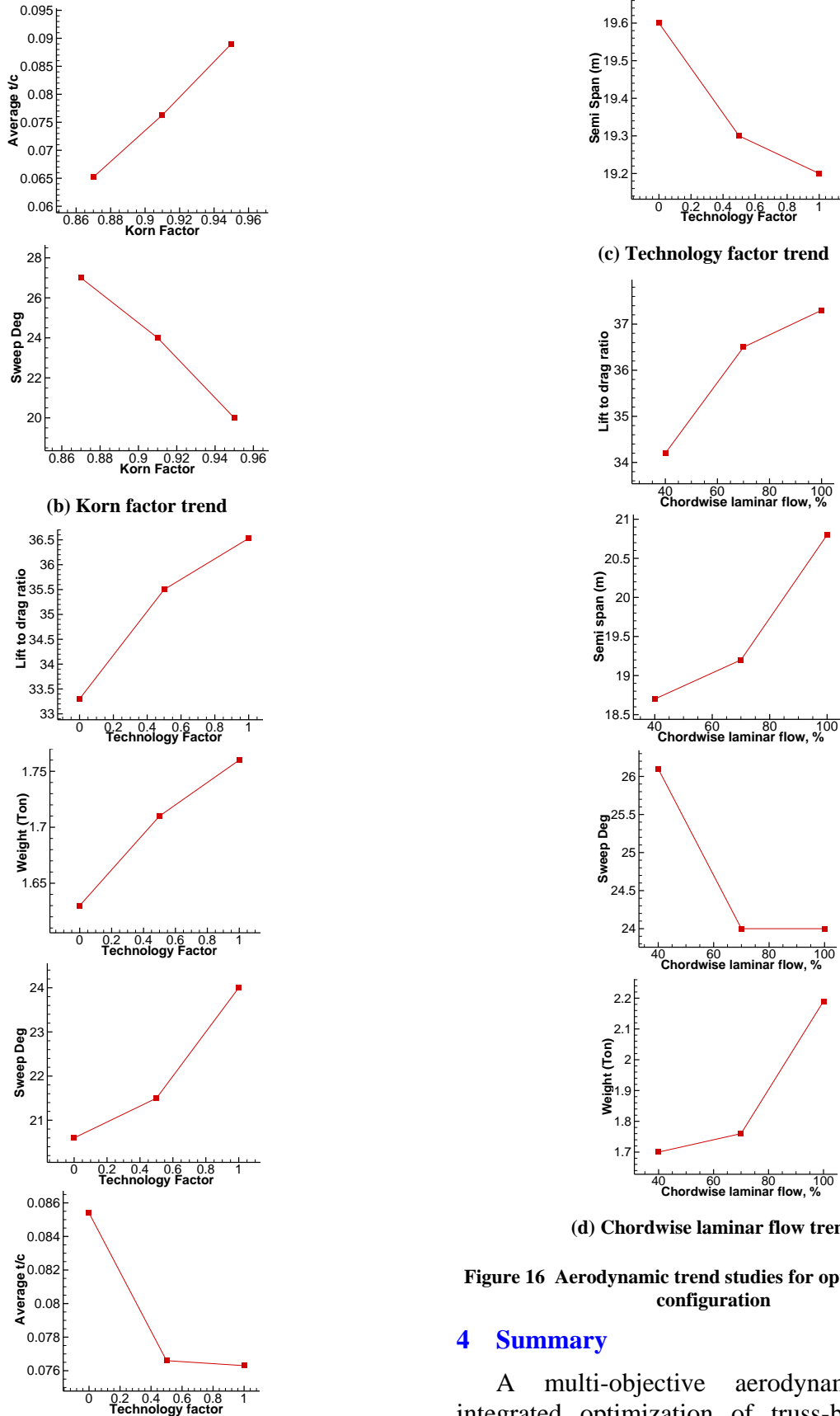


Figure 16 Aerodynamic trend studies for optimum TBW-2 configuration

#### 4 Summary

A multi-objective aerodynamic/structure integrated optimization of truss-braced wing (TBW) configuration are conducted in this paper. The interference drag between wing and strut, strut and fuselage, strut and strut is

predicted by inviscid Euler simulation; for structural discipline, the box-beam model is used and full-stress optimization is utilized for sizing. The Pareto fronts are obtained for maximizing L/D and minimizing weight for strut-braced wing (SBW), TBWs with one and two juries. It is shown from this study and the TBW-2 with two juries holds the highest benefit of increasing aerodynamic L/D and reducing structural weight. An aerodynamic trend study is conducted for TBW-2 configuration, which shows the aerodynamic features of the optimum and the benefit of TBW could be further exploited by refined MDO framework.

## 5 Acknowledgements

The authors would like to acknowledge the financial support of National Natural Science Foundation of China (NSFC) under grant No. 11272265.

## 6 References

- [1] Bradley, M. K. and Droney, C. K., "Subsonic ultra green aircraft research: phase I final report". NASA/CR-2011-216847, 2011.
- [2] Pfenninger, W. Laminar flow control laminarization. AGARD Rept. 654, Neuilly-sur-Seine, France, 1977.
- [3] Grasmeyer, J.M. Multidisciplinary design optimization of a strut-braced wing aircraft. *Virginia Polytechnic Institute and State University, Master thesis*, 1998.
- [4] Gern, F.H., Ko, A., Grossman, B., Haftka, R., Kapania, R.K. and Mason, W.H. Transport weight reduction through MDO: the strut-braced wing transonic transport. AIAA Paper 2005-4667, 2005.
- [5] Gur, O., Bhatia, M., Schetz, J. A., Mason, W. H., Kapania, R.K., and Mavris, D. N., "Design optimization of a truss-braced-wing transonic transport aircraft," *Journal of Aircraft*, 2010, Vol.47, No.6, pp. 1907-1917.
- [6] Meadows, N. A., Schetz, J. A., Kapania, R. K., Bhatia, M., and Seber, G., "Multidisciplinary Design Optimization of Medium-Range Transonic Truss-Braced Wing Transport Aircraft," *Journal of Aircraft*, 2012, Vol.49, No.6, pp.1844-1856.
- [7] Horstmann, K. H., "Ein Mehrfach-Traglinienverfahren und seine Verwendung für Entwurf und Nachrechnung nichtplanarer Flügelanordnungen", DFVLR-FB 87-51, 1987.
- [8] Lamar, J. E., "A Vortex Lattice Method for the Mean Camber Shapes of the Trimmed Non-Coplanar Platforms with Minimum Vortex Drag," NASA TN D-8090, June, 1976.
- [9] Khan, F. A., "Preliminary Aerodynamic Investigation of Box-Wing Configurations using Low Fidelity Codes", Master's Thesis, Luleå University of Technology, Sweden.
- [10] Grasmeyer, J. M., Naghshineh, A., Tetrault, P.-A., Grossman, B., Haftka, R. T., Kapania, R. K., Kapnia, R. K., Mason, W. H., Schetz, J. A., "Multidisciplinary Design Optimization of a Strut-Braced Wing Aircraft with Tip-Mounted Engines," MAD Center Report, MAD 98-01-01, January 1998.
- [11] Mason, W. H., FRICTION Code Documentation, available on the World Wide Web at: [http://www.aoe.vt.edu/aoe/faculty/Mason\\_f/CatxtAppD5.pdf](http://www.aoe.vt.edu/aoe/faculty/Mason_f/CatxtAppD5.pdf).
- [12] Braslow, A. L., Bartlett, D. W., Wagner, R. D., and Collier Jr., F. S., "Applied Aspects of Laminar-Flow Technology," Viscous Drag Reduction in Turbulent Boundary Layers, edited by D. M. Bushnell and J. N. Hefner, Vol. 123, Progress in Aeronautics and Astronautics, AIAA, New York, 1990.
- [13] Ravi K. Duggirala, Christopher J. Roy, and Joseph A. Schetz, "Analysis of the Interference Drag for Strut-Strut Interaction in Transonic Flow", 47th AIAA Aerospace Science Meeting, Jan 2009.
- [14] Gur, O., Schetz, J. A., and Mason, W. H., "Aerodynamic Consideration in the Design of Truss-Braced Wing Aircraft", 28th AIAA Applied Aerodynamic Conference, Chicago, Illinois, July 2010.
- [15] Liu, J., Han, Z. -H., and Song, W. - P., "Efficient Kriging-based Optimization Design of Transonic Airfoils: Some Key Issues.," AIAA 2012-0967, 50th AIAA Aerospace Sciences Meeting, Jan.9-12, 2012, Nashville, Tennessee.
- [16] Han, Z. H., Zhang, K. S., Liu, J., and Song, W. P., "Surrogate-based Aerodynamic Shape Optimization with Application to Wind Turbine Airfoils," AIAA Paper 2013-1108, Jan. 2013.
- [17] Sacks, J., Welch, W. J., Mitchell, T. J., and Wynn, H. P., "Design and Analysis of Computer Experiments," *Statistical Science*, Vol. 4, 1989, pp. 409-423.
- [18] Deb, K., Agarwal, S., and Meyarivan, T., "A fast and elitist multiobjective genetic algorithm: NSGA-II," *Evolutionary Computation*, 2012, Vol. 6, No. 2, pp. 182 - 197

## 7 Contact Author Email Address

Mailto: zhangkeshi@nwpu.edu.cn

## 8 Copyright Statement

The authors confirm that they, and/or their company or organization, hold copyright on all of the original material included in this paper. The authors also confirm that they have obtained permission, from the copyright holder of any third party material included in this paper, to publish it as part of their paper. The authors confirm that they give permission, or have obtained permission from the copyright holder of this paper, for the publication and

distribution of this paper as part of the ICAS 2014 proceedings or as individual off-prints from the proceedings.